UNIVERSITY OF CALIFORNIA SAN DIEGO

Modeling Human Retinal Ganglion Cell Development and Connectivity

A thesis submitted in partial satisfaction of the requirements for the degree Master of Science

in

Biology

by

Cairang Jia

Committee in charge:

Professor Karl J. Wahlin, Chair

Professor Yimin Zou, Co-Chair

Professor Alysson R. Muotri

Professor David Traver

Professor Karl Willert

2021

The thesis of Cairang Jia is approved, and it is acceptable in quality and form for publication on microfilm and electronically.

University of California San Diego

2021

Dedications

Dedicated to all my family, friends and researchers around the world sharing the same dream with me.

Table of Contents

List of Figures and Tables

Acknowledgements

I would like to thank all Wahlin Lab members for their unwavering support and sharing so much joy and tears with me. I cannot be more grateful about working in such a beautiful environment filled with truthful love.

I would also like to thank Dr. Alysson Muotri and Muotri Lab member Jason Adams for their profession guidance and collaboration. Only with their support can I accomplish all these experiments.

Lastly, I would have my most sincere gratitude to Dr. Karl Wahlin for all the guidance across my research journey while being an amazing friend with me. I'll always be grateful for all the invaluable advice and joyful memories we had together.

ABSTRACT OF THE THESIS

Modeling Human Retinal Ganglion Cell Development and Connectivity

by

Cairang Jia

Master of Science in Biology

University of California San Diego, 2021

Professor Karl J. Wahlin, Chair
Professor Yimin Zou, Co-Chair

In humans, retinal ganglion cell (RGC) loss, as occurs in glaucoma, is irreversible and leads to permanent loss of vision. Endogenous regeneration, the process whereby new neurons are created from existing glial cells, offers one possible approach to address this condition. For this approach to succeed, there is still much that needs to be learned about RGC during development. To address this, carried out three lines of research including (1) human pluripotent stem cell derived retina/brain co-culture experiments to evaluate axon targeting, (2) WNT agonist treatments

to improve retinal organoid differentiation, and (3) direct conversion of RGCs from pluripotent stem cells to explore how axons project from the eye to the brain. For co-culture experiments, retinal organoids were complexed with thalamus and cortical organoids. RGCs showed substantial axon neurite outgrowth induced by conditions provided by thalamus and cortical organoids. For experiments designed to improve differentiation, different concentrations of the WNT agonist CHIR99021 were tested on developing retinal organoids at different time points. Treatments from days 16 to day 22 showed generally improved retinal vesicle quality. Based on ongoing work in the lab aimed at exploring direct conversion to probe transcription factors important for RGC development, overexpression of NEUROG2, ATOH7, ISL1, and POU4F2 were shown to differentiate iPSCs into RGCs. Using this approach, I developed inducible neurons with and without retinal ganglion cell qualities. Overall, these new tools and concepts will provide new insight into human retinal ganglion cell development.

Introduction

Eye Development and Retinogenesis:

In early embryogenesis, the neural plate invaginates to form the neural groove. Shortly after, neural folds, on each side of the neural groove, move toward each other and eventually form the neural tube, which is the origin of our central nervous system (CNS). A variety of factors, including WNT, Retinoic acid and HOX genes, functions to pattern our CNS into different compartments(Carroll, 1995; Elkouby and Frank, 2010; Kiecker and Niehrs, 2001). The developing CNS can be generally classified into telencephalon, diencephalon, mesencephalon, metencephalon, myelencephalon and spinal cord. Specifically, the diencephalon is the structure that involved in eye development and will eventually give rise to anterior multiple forebrain structures, including thalamus, hypothalamus, posterior pituitary, and pineal gland. On each side of the diencephalon, optic vesicles will bulge out and extend outward toward epithelium tissue(Fuhrmann et al., 2000a). At their exterior end, optic vesicles will invaginate and form bilateral positioned optic cups(Hyer et al., 2003). The inner layer of optic cup will give rise to retina while the outer layer will differentiate into retinal pigmented epithelium (RPE), a dark pigmented layer of tissue with photoprotective functions and responsible for completing visual cycle to replenish photoreceptors with molecules for photo-transduction. The hollow tissue between optic cup and diencephalon will form optic stalk, which is the pathway of optic nerve. Out of all retinal neurons, retinal ganglion cells (RGCs) form in the early stage of retinogenesis. Axons of RGCs will bundle together to form the optic nerve, passing through optic stalk and reach optic chiasm. At optic chiasm, about half of optic nerve will cross from ipsilateral side to contralateral side in human(Kupfer et al., 1967). Optic nerves eventually connect to dorsal lateral

geniculate nucleus (dLGN) in ventral thalamus, which then connect to visual cortex and form the complete visual circuit(Martin, 1986).

The retina is a well-organized structure with complex lamination to facilitate the ocular signal transduction (Figure 1). On the very top of the retina sits the photoreceptor cells, which includes both rods and cones. Those cells are responsible for photo-detection. Cell bodies of photoreceptors form outer nuclear layer (ONL). Photoreceptors innervate with horizontal cells and bipolar cells, forming the outer plexiform layer (OPL). Bipolar cells in turn connect with amacrine cells and RGCs, forming the inner plexiform layer (IPL). Cell bodies of horizontal, amacrine and bipolar cells form the inner nuclear layer (INL), while ganglion cell bodies form the ganglion cell layer (GCL). The retinal architecture is maintained by Müller Glia cells, which span the width of the retina from the inner, near RGCs, to the outer limiting membrane (near photoreceptors).

Retinal Ganglion Cell Connectivity In vivo:

RGCs convey signals from the retina towards higher order neurons in brain, targeting lateral geniculate nucleus (LGN), suprachiasmatic nucleus (SCN), superior colliculus (SC) and olivary pretectal nucleus (OPN), with each structure in charge of specific functions. Most RGCs project to the LGN in the ventral thalamus, which is the relay station for the visual cortex and is responsible for much of our image forming capability(Martin, 1986). A small population of RGCs also consists of intrinsically photosensitive retinal ganglion cells that control circadian rhythms(Berson, 2003). This unique type of RGC is photosensitive, conducting their signal to SCN in the hypothalamus and OPN in the midbrain. The SCN pathway further relay its signal to the pineal gland, regulating our circadian rhythm(Colwell et al., 2004). The OPN pathway directly controls our pupillary reflex to help our eyes adjust to ambient light level(Keenan et al., n.d.). Some RGCs also project to the superior colliculus in the midbrain, providing the body with a sense

of head position as well as regulating head and eye movement(Pierrot-Deseilligny et al., 2003). However, the development of those connections is not well understood since humans, particularly at fetal stages, are not experimentally accessible.

Human iPSCs Derived "Organoid" Technology:

To circumvent the moral burdens surrounding *in vivo* human research, "organoid" technology has been utilized in a variety of biomedical fields to model human development and diseases(Lancaster et al., 2013; Sato et al., 2009). Multiple reports have shown that organoids closely mimic *in vivo* development and displayed similar gene expression profiles(Camp et al., 2015; Sato et al., 2009). Different groups have also reported organoids possess similar activity as observed *in vivo*, including spontaneous network firing of neurons in cortical organoids(Trujillo et al., 2019). Due to its close resemblance in physiology *in vivo,* organoids are well suited to study development and disease for many tissues and organs. However, the other side of the coin is organoid's close mimicry to human development sometime means extremely long cell culture timing which takes about 9 months, or longer, in humans. The time-consuming nature of human development might make it hard for fast and scalable experimental design as well as trouble shooting. In addition, cell line variability exists, and this can prevent some lines from differentiating into a given cell or tissue type. In addition, organoids' variability can sometimes observed in different batches and even within the same batch receiving same treatment(Quadrato et al., 2016). When it comes to data analysis, fluorescent cell-type specific reporters offer one way to reduce variability. The use of reporters is particularly useful when co-culturing multiple organoid types, such as a visual circuit comprised of retina, thalamus, and visual cortex organoids.

Visual Signal Transduction:

The visual pathway starts in the retina when photons of light reach photoreceptors. Upon light activation of opsins, membrane channels open and hyperpolarize the membrane which then blocks glutamate release. Visual information is processed by lateral inhibition modulated by horizontal cells to boost the image contrast before it is sent to bipolar cells(Thoreson and Mangel, 2012). Bipolar cells then relay neuronal impulses to amacrine cells for lateral inhibition again before relaying this information to RGCs(Bloomfield and Xin, 2000). RGC axons bundle together to form the optic nerve, which extends into dorsal lateral geniculate nucleus (dLGN) in ventral thalamus(Kupfer et al., 1967). Dorsal LGN mainly consists of magnocellular cells, parvocellular cells and koniocellular cells(Jeffries et al., 2014). The magnocellular pathway mainly processes fast moving objects with good spatial resolution signal received from rod photoreceptors(Pokorny, 2011). The parvocellular pathway processes color information with fine details received from long and medium wavelength opsin expressing cone photoreceptors(Xu et al., 2001). Koniocellular cells are mainly responsible for processing blue light signals received from short wavelength opsin expressing cone photoreceptors(Xu et al., 2001). Then dLGN then relays the information processed by magnocellular and parvocellular cells towards the visual cortex for higher order processing, ultimately giving us vision. Given the integrated nature of the visual circuit, a single isolated organoid cannot recapitulate the whole pathway. Therefore, a retina, thalamus and cortex co-culture assembloid was proposed to reconstitute the visual circuit *in vitro*. Human retinal organoid (RO) and cortical organoid (CO) have been used extensively in the field to study neural developments and pathologies(Lancaster et al., 2013; Setia and Muotri, 2019; Wahlin et al., 2017). A thalamus organoid (ThO) system was only recently introduced(Xiang et al., 2019). The co-

culture of three organoids will offer meaningful insight into optic nerve and brain neural plasticity *in vitro*.

Medium Wavelength Opsin Optogenetic Tool:

In retinal organoids, RGCs are the first cells to develop, appearing around day 35 (Figure 2). However, essentially all retinal organoid systems suffer from significant late stage RGC loss, which is irreversible (Figure 2). Photoreceptors and bipolar cells are usually observed in retinal organoid cultures after day 100(Wahlin et al., 2017). Thus, as photoreceptors start to mature, the RGCs begin to die. Therefore, a major challenge is to form a complete retina that is capable of visual transduction from photoreceptors to RGCs. To circumvent this limitation and allow exploration of the role of light in shaping the visual circuit, we wanted to make our retinal organoids light-sensitive at early stages. To do this, iPSCs were engineered using CRISPR/Cas9 to express medium wavelength cone opsin (MWopsin), rendering it activatable by green light(Berry et al., 2019). Different from the classic Channel Rhodopsin optogenetic model, the MWopsin system is most sensitive to dim green light, instead of high intensity blue, and functions with high frequency, sensitivity and spatial and temporal resolution in mice(Berry et al., 2019). Upon eradication of photoreceptors, viral delivery of MWopsin successfully recovered light sensitivity as well as light pattern discrimination *in vivo*(Berry et al., 2019). Though only responsive to green light, MWopsin active RGCs can fire more frequently, thus offering better temporal resolution for vision.

Transcription Factors Involved in Retinogenesis:

Transcription factors play indispensable roles in retinal development. For instance, SIX6 serves to maintain retinal progenitors cell population to facilitate retinal differentiation and was

genetically modified by our lab to co-express with a green fluorescent protein to better identify live retinas in real-time(Diacou et al., 2018) (Figure 2). For retinal ganglion cells, a variety of transcription factors, including NEUROG2, ATOH7, ISL1, POU4F1 and POU4F2 are responsible for inducing retinal ganglion cell development during retinogenesis as well as driving differentiation of different RGC subtypes(Hufnagel et al., 2010; Wu et al., 2015). At early stages of eye development, Notch signaling activates waves of proneural gene expression, leading to retinal neurons that differentiate at different stages (Artavanis-Tsakonas et al., 1999). In the retina, Notch pathway induce expression of ATOH7, a key factor in RGC fate determination(Maurer et al., 2014). ATOH7 further regulates the downstream transcription factors ISL1 and POU4F2. ISL1 and POU4F2 were reported to be sufficient for converting retinal progenitor cells into RGCs *in vivo*(Wu et al., 2015). While POU4F2 is essential for RGCs survival and maintenance, ISL1 functions to keep POU4F2 stably expressed to ensure a healthy RGC population(Mu et al., 2008).

POU4F1-3, commonly known as BRN3A-C, are the most widely used markers for identifying RGCs(Badea et al., 2009; Nadal-Nicolás et al., 2009). In humans, POU4F1 and POU4F2 are expressed in about 80% of RGCs with significant amount overlapping expression, whereas POU4F3 is only expressed in 20% of RGCs (Xiang, 1998; Xiang et al., 1995). This family of transcription factors is essential for RGC development. POU4F1 is not only important for RGC development, but also indispensable for the development of a variety of other central and peripheral neural structures, including dorsal root ganglia, spinal cord, red nucleus, superior colliculus, and motor neurons(Fedtsova and Turner, 1995; Zou et al., 2012). POU4F1 knockout mice reportedly die at birth due to CNS defects (McEvilly et al., 1996). On the other hand, POU4F2 knockout mice develop with substantially fewer RGCs, though many of these survive, possibly from compensation by POU4F1 and POU4F3. Double POU4F1/POU4F2 or POU4F2/POU4F3

knockouts displayed much worse phenotype than single knockout of POU4F2, showing that this family of transcription factors cooperates to regulate RGC development(Wang et al., 2002).

Transcription factors also play an important role in retinal regeneration. Mature mammals generally do not possess the ability to regenerate retinal neurons once damaged. In damaged mouse retinas, Müller Glia cells(MGs) enter a reactive phase, involving gliosis which leads to scar tissue formation and partial vision loss (Dyer and Cepko, 2000). However, it was found that adult mouse MG could regenerate retinal neurons after damage if particular transcription factors were activated by gene overexpression or microRNA control(Guimarães et al., 2018; Pollak et al., 2013; Wohl et al., 2019). In those reports, genetically edited MG cells in damaged retinas first undergo de-differentiation, entering a state in which their expression profile mimics retinal progenitor cells(Pollak et al., 2013). Increasing NEUROG2 or ASCL1 expression induces MG to differentiate into retinal neurons(Wohl et al., 2019). Newly derived retinal neurons included photoreceptor, bipolar, RGCs and amacrine neurons. This endogenous regeneration approach offers great potential for vision restoration. Therefore, it is worthwhile exploring best culturing conditions to derive specific type of neurons, in this case RGCs, by temporarily overexpressing essential transcription factors with our Tetracycline inducible system *in vitro*.

2D Direct-Conversion Neuron Culture:

Direct conversion of iPSCs can generate certain cell types much faster than organoid cultures, enabling scalable experiments with faster turnaround time. Direct-conversion typically involves overexpression or downregulations of certain genes or RNAs. Our lab has found that RGCs can be directly converted from iPSCs with ~35% efficiency (Figure 9) in 2D cultures simply through overexpressing a combination of transcription factors, including NEUROG2, ISL1, ATOH7 and POU4F2 (NAIB). Astonishingly, overexpressing NEUROG2 alone can generate

more general neurons with a frequency approaching 100% (Figure 10A-B). Using the overexpression system mentioned above, I introduced the NAIB transcription factors above into a POU4F2-tdTomato reporter iPSC line also expressing an optogenetic MWopsin switch. In parallel, I also generated a GCAMP6s iPSC line and similarly introduced a NEUROG2 gene alone. Both lines were subsequently converted into neurons in 2D cultures to verify their function *in vitro*. The GCAMP6s calcium indicator system possesses unique advantages of high sensitivity to calcium concentration with slow decay, ideal for visualizing live neuron activity, which experiences drastic calcium influx during action potential(Chen et al., 2013).

WNT Pathways' Involvement in Eye Development:

Canonical WNT signaling plays multiple roles in development, particularly in the developing nervous system. In embryonic stages, WNT acts as a caudalizer in the antero-posterior axis to pattern the central nervous system(Elkouby and Frank, 2010). Like other important morphogens, a gradient of WNT is essential for proper formation of neural compartments. WNT's also play important roles in eye development. Knockout of β-catenin, an essential protein of WNT pathway, disrupts lens placode development(Smith et al., 2005). At early stages, WNT pathway is also active for corneal induction, which is achieved through BMP4 pathway inhibition(Nakatsu et al., 2011). In addition, WNT signaling is important for development and maintenance of retinal pigment epithelium (RPE), a layer of pigmented cells adjacent to the retina(Fuhrmann et al., 2000b). In contrast, WNT activity is strictly inhibited in the central mature retina and only active at the ciliary margin(Chen et al., 2008; Kreslova et al., 2007). Despite the inhibitory role at early stages, it is also reported that WNT signaling patterns the dorsal-ventral directionality of retina during development(Veien et al., 2008; Zhou et al., 2008). Here, we used WNT agonist

CHIR99021 to study how can we apply WNT signal at appropriate time point to make better retinal organoids.

Results and Discussions

CHIR99021's Effect on Retinal Development

It is well known that WNT signaling is important for neural development, and retinal development is no exception. To investigate the role WNT signaling during optic vesicle formation, we applied the WNT agonist CHIR99021 at different stages of development. Controls receiving no CHIR produced small and thin vesicles with relatively weak SIX6-eGFP expression on day 25. While containing a number of retinal vesicles, the control group also generated some transparent vesicles, which closely mimicked corneal and possibly choroid plexus tissues based on morphology. These were not further studied. Groups that received CHIR at the earliest period from days 8-12 or days 10-14 displayed no SIX6-eGFP expression at all, indicating a failure to derive optic vesicles (Figure 5). WNT signaling act as a caudalizer in the early neural development, so this result was not surprising(Elkouby and Frank, 2010). Therefore, we believe that WNT treatments induced mid-to-hindbrain formation(Kim et al., 2018). Groups treated with CHIR from days 12-16 and days 14-18 yielded small amount of SIX6 positive retinal vesicles, with most vesicles still being SIX6 negative (Figure 5). On the other hand, groups treated with CHIR from days 16-20 and 18-22 displayed robust SIX6-eGFP expression that gave rise to optic vesicles with excellent morphology (Figure 6). Finally, groups treated with CHIR from days 20-24 gave rise to thin optic vesicles with relatively weak SIX6-eGFP expression along with some transparent structures similar to controls, indicating WNT signaling was not be able to significantly impact retinal

development after 20 days of differentiation following our protocol. In conclusion, CHIR treatments from days 16-20 and 18-22 significantly improved retinal vesicle quality, which allowed me to produce large numbers of high-quality optic vesicles for retina-thalamus-cortex assembloid experiments.

RO-ThO-CO Assembloid

The overarching goal of my project was to recapitulate the whole visual circuit and study RGCs' neural plasticity during development. And to do this I set out to establish a tri-assembloid system with 3 different types of organoids representing each component of a human visual circuit. 3D retinas were generated using our laboratory's custom protocol, using IMR90.4 SIX6-GFP / POU4F2-tdTomato-Medium Wavelength Opsin optogenetic iPSCs, which upon differentiation displayed robust levels of red fluorescence in RGC axons (Figure 4) which greatly assisted with the tracing of optic nerve growth. Thalamus organoids, in an IMR90.4 background expressing GCAMP6s, were generated based on published protocols by Xiang et al with minor modifications described in the methods section (Xiang et al., 2019) (Figure 3). Cortical organoids in the wt83 background were provided by Dr. Alysson Muotri's laboratory by graduate student Jason Adams in an ongoing collaboration. In order to link the three organoids together, gravity-induced fusion was established over 48 hours on tilted plates (see method). Robust RGCs axon outgrowth was observed 3 days after initialization of fusion, extending into and even beyond thalamus organoids to extend into cortical organoid (Figure 4). Established Axon remained up to three weeks before committing to apoptosis with loss of lamination and RGCs' axon from ROs (data not shown). Across the whole experiment, little to no cell body migration was observed, with all organoids remained inside their boundaries and maintained their identity. Overall, our studies demonstrated that we were able to co-culture organoids from three discrete regions of the CNS and that they

could make morphological connections. Future work should resolve whether functional connections are made by using a combination of techniques including live cell calcium imaging, microelectrode arrays (MEAs), and single cell electrophysiology.

Media Choice of RO-ThO-CO Assembloid

After testing LTR, TDM, and modified Muotri Lab cortical media 2, we found that LTR and TDM have the tendency to cause organoids deteriorate quickly. Modified cortical media 2 (Neurobasal supplemented with 1x GlutaMAX, 1x B27, 1x NEAA) was found to be best suited for all three types of organoid the best during co-culture with simplest recipe and was used in feeding every day(Trujillo et al., 2019).

Assessing induced retina ganglion (iRGC) cell generation in Normoxia and Hypoxia.

Direct-conversion of neurons from iPSCs is a scalable way to study neurons *in vitro*. The main advantage is that it dramatically reduced the time necessary to generate human retinal ganglion cells. In typical 3D generated retinal organoid cultures, RGCs usually start to develop around day 35. In contrast, previous and current lab members (Ryan W. Wong and Nicholas Dash) established that transcription factor mediated iRGCs generation yielded RGCs in as little as 4-6 days in 2D culture. Oxygen level can influence differentiation in significant ways. Many labs grow pluripotent stem cells under normoxia (5%Co2, 20%O_2) or hypoxia (10CO2, 5%O2). Here, I tried to explore the best culturing condition with the overexpression system, testing conditions that include normoxia vs hypoxia, with or without treatment of SB431542, a potent TGF-β inhibitor, on day 0 and the choice of media used for culture.

Control cells included a Tet inducible system cassette lacking transcription factors for overexpression. Group 1 cells possessed the Tet inducible system and only NEUROG2 in the

overexpression component. Group 2 cells possessed Tet inducible system and a cocktail of the 4 NAIB transcription factors in the overexpression component.

In all conditions, the control line displayed no neural morphology, with the whole plate covered by flat cells with protrusions (Figure 9). For the NEUROG2 cell line, direct-conversion culture yielded some neurons, with numeral axons forming a meshwork on the plate, but still contained some non-neural flat cells (Figure 9). Lastly, the NAIB line showed that most cells differentiate into neurons with only a few flat cells sparsely distributed (Figure 9).

Under all conditions, control cells displayed no neural or RGC differentiation (Figure 7-9). Under hypoxia, NEUROG2 overexpression yielded 17±2% efficiency for POU4F2-tdTomato+ detection while NAIB overexpression achieved higher 34 ±7% direct-conversion efficiency, which was statistically significant with a p-value of 0.016 (Figure 9). Under normoxia, NEUROG2 overexpression yielded 11±2% and NAIB achieved 29±6% direct-conversion efficiency (Figure 9), which was also statistically significant with a p-value of 0.007. Overall, hypoxic condition was slightly more efficient for generating NEUROG2 and NAIB POU4F2-tdTomato+ neurons.

2D Derivation of Optogenetic RGCs and Gcamp6s Neurons

With the advantage of our transcription factor expression system, I developed an induced neuron approach to generate medium wavelength opsin optogenetic RGCs and neurons with GCAMP6s, integrated into a genomic safe harbor site, to study activity dependent function of RGCs. IMR90.4 iPSCs with GCAMP6s integrated were transfected with a NEUROG2 overexpression plasmid and zeocin selected to achieve a pure population. IMR90.4 optogenetic MW opsin cells were also transfected with the 4 factor NAIB overexpression plasmid, which were similarly selected to purity by zeocin selection. After zeocin selection, cells were propagated and

differentiated based on our 2D direct-conversion protocol (see method). Unlike previous experiments in IMR90.4 POU4F2-tdTomato cell line, 2D culture of optogenetic RGCs from iPSCs yield a very small amount of RGCs, potentially due to aberrant changes during gene editing that have yet to be understood. 2D culture of GCAMP6s neurons, however, yielded close to 100% neurons, forming a mesh-like network on the plate (Figure 10A-B). When not activated, weak green fluorescence was observed in the cell body (Figure 10E). Upon a treatment of 50mM KCl, Day 4 GCAMP6s neurons displayed robust fluorescent axons, indicating gcamp6s is function in our 2D derived neurons (Figure 10F). While additional work is required to show functional networks between MW-opsin iRGCs and GCAMP+ NEUROG2 induced neurons the work highlighted here demonstrates sufficient proof-of-principle results and lays the foundation for functional studies between RGCs and GAMP responsive target cells. This would be helpful as a quality control measure to assess functional activity of other transcription factor cocktails.

Methods

Plasmid Construct

POU4F2-tdTomato-MWopsin cell line was constructed based on POU4F2-tdTomato plasmid made by previous lab member (Anna Ogata). The plasmid was linearized at the point behind tdTomato fluorescent gene and amplified using PCR. Medium wavelength opsin gene was obtained from RNA extracted from a mature retinal organoid. After obtaining RNA, cDNA library was generated from the RNA extraction. And MWopsin gene is specifically amplified using PCR

with corresponding oligos. Oligos used to amplify MWopsin and linear POUF2-tdTomato were specifically designed to have overlapping regions.

Then, the linearized POUF2-tdTomato and MWopsin was integrated using Gibson Assembly Technique. After, the Gibson assembled product was DPN1 digested and transformed into competent stable E. Coli (#C3040I; NEB). Multiple E. Coli colonies were then cultured and subjected to Zymopure Mini Prep plasmid purification (#D4209; Zymo Research). The purifications were then Sanger Sequenced and selected if no significant mutation was found.

CLYBL-GCAMP6s (slow plasmid) was previously made in the lab, however, a deletion in the Cbh promoter rendered it less effective. To fix this promoter, a copy of Cbh promoter with no mutation was PCR amplified. Then, PCR amplified Cbh promoter and original Gcamp6s plasmids were restriction digested with Mlu1 and Asel1 restriction enzyme, yielding blunt end. Lastly, digested Cbh promoter and Gcamp6s backbone were ligated together with T4 ligation (#M0202S; NEB). The correction was verified by Sanger sequencing using a power-read service (Eurofin) to overcome GC rich complexity related sequencing problems.

Stem Cell Maintenance

IMR90.4 iPSCs were used for experiments. Stem cells were fed with mTeSR1 (Stem Cell Technologies) on 1% (vol/vol) Matrigel (MG)-GFR™ (#354230; BD Biosciences) coated Tissue-Culture-Treated dishes at 37°C under hypoxia (5% O_2 and 10% CO_2) or normoxia (20% O_2 and 5% CO_2) upon need for specific experiments.

Passaging was executed with Accutase (#A6964; Sigma) for 12 minutes at 37°C. Then, the single cell suspension was quenched with mTeSR1 supplemented with 5μM blebbistatin (B; #B0560; Sigma). After, quenched suspension was pelleted at 80xg for 5min. Cells were then

counted and plated with appropriate density in mTeSR1 supplemented with 5μM blebbistatin. Feeding with mTeSR1 resumed 2 days after plating. In addition, iPSCs were routinely tested for mycoplasma.

Plasmid Preparation for Stem Cell Transfection

Plasmids were purified with the PureLink Fast-Low Endotoxin Midi Plasmid Purification Kit (#210015; Invitrogen). To prevent unwanted degradation of DNA, plasmids used for transfection were never thawed more than three times.

Electroporation Transfection

For reporter cell generation (POU4F2-p2A-tdTomato-p2A-MWopsin), IMR90.4 iPSCs with stable integration of GFP at the endogenous SIX6 gene and Tet-inducible Cas9 system at the AAVS1 locus were pretreated with doxycycline at 1μg/ml for 24 hours. For iPSCs used for overexpression cassettes we did not treat with doxy since that would initiate gene expression prematurely. After 24 hrs, cells were Accutase (#A6964; Sigma) treated for 12 minutes at 37°C. The single cell suspension was then quenched with mTeSR1 plus 5μM blebbistatin (B; #B0560; Sigma), pelleted at 80xg for 5 minutes, and resuspended in mTeSR1 plus 5μM blebbistatin (B; #B0560; Sigma). 200,000 cells were transferred to a 1.5ml tube and pelleted at 80xg for 5 minutes again. After pelleting, the cell-less suspension was aspirated and chilled on iced for 20 minutes for maximal survival. Cells were quickly resuspended in 12μl of resuspension buffer containing 3μg total plasmid, followed by electroporation with a Neon transfection system (#MPK5000; Invitrogen) at 1300V, for 20ms. For iPSCs designed for overexpression (CLYBL-GCAMP6s, NRGN2, NAIB), we used two plasmids (1) a CLYBL site donor equipped with a 3G-Tet promoter and a zeocin selection cassette and (2) a plasmid containing a CRISPR-Cpf1 and a tracr sequence

targeting the CLYBL safe harbor site. After transfection, cells were evenly plated on Matrigel (#354230; BD Biosciences) coated 12 well plates in mTeSR plus 5μM blebbistatin (B; #B0560; Sigma). After 48 hours, feeding with mTeSR1 resumed.

Genotyping of Transfected Reporter Cells

After iPSCs colonies reached a size equivalent to 75% of a field of view on 10x objective, a cell scraper was used to lift colonies into suspension. In the first pass of genotyping, 4-5 colonies were transferred into a well on Matrigel coated 48 well plate to maximize chance of getting colonies with desired insertion. After colonies reached decent size on 48 well plate, another round of CDB passaging was performed, which 95 percent of suspension would be used for PCR verification and 5% would be re-plated on a new Matrigel coated 48 well plate. For all cloning and genotyping procedures, we used Phusion Flash polymerase according to the manufacturer's guidelines. The oligonucleotides (see table 1) used for first pass PCR verification consisted of one oligo outside the insertion site and one oligo inside the insertion, testing for if insertion happened or not. Wells with positive results from verification were then Accutase passaged onto Matrigel coated 12 well plate and further selected to ensure homogeneity.

In the second round of genotyping, the colonies were scraped again and only one colony was transferred into each well of Matrigel coated 48-well plate to ensure purity. After colonies reached 75% of a field of view (10X objective), cells were CDB passaged again, with ~95 percent of suspension used for PCR verification and ~5% (~1 drop) was re-plated onto a new Matrigel coated 48 well plate. The oligo set (see table 1) using for second pass PCR verification consisted of 2 oligos outside the insertion site, testing for homozygous insertion or heterozygous insertion. Homozygous insertion displayed a bright band at larger size on electrophoresis gel. Heterozygous insertion displayed two equally bright band at different sizes. Homozygous no insertion had a

bright band at smaller size. Homozygous inserted colonies were then propagated and sequence for mutations before using in experiments.

2D Tet-inducible Neuron Direct-Conversion

The goal of this experiment was to explore best culture conditions for inducing RGC direct conversion from our gene edited iPSCs. For this, cells were grown in Brainphys (#05790; Stemcell Technologies) with 1x B27 (#17504044; Invitrogen). The 3 cells lines used for experiments were IMR90.4 SIX6-eGFP POU4F2-tdTomato transfected with a Tet-inducible backbone, Tet-inducible NEUROG2 and Tet-inducible NAIB. Cell lines were maintained in both hypoxia (5% O_2 and 10% CO_2) and normoxia (20% O_2 and 5% CO_2). GCAMP6s cells were transfected with Tet inducible NEUROG2 and maintained in hypoxia, following by 2D direct conversion in the same fashion.

The day before experiment, 6 well plates were treated with poly-ornithine (PLO) overnight. One the second day, the PLO treated wells were aspirated and washed three times with distilled water, following by drying for an hour. Plates were then coated with Matrigel for no less than 3 hours.

Cells were maintained on 6 well plate to approximately 50% confluency and pretreated with 0.5μg/ml doxycycline plus100nM LDN193189(#SML0559; Sigma) and/or 10μM SB431542 (depending on treatment groups, #14775S; Cell Signaling). Once day later, cells were Accutase passaged and resuspend in Brainphys media supplemented with 1x B27, 1μg/ml doxycycline, 5μM blebbistatin, 100nM LDN, 1:100 CultureOne (#2283831; Gibco) and with or without 10μM SB431542. Resuspended cells were passed through 35 micro filter to reduce cell clumps. 72,000 of cells were plated on PLO and Matrigel coated 6 well plates in BrainPhys media supplemented

with 1x B27, 1μg/ml doxycycline, 5μM blebbistatin, 100nM LDN, Culture one (1:100) and with or without 10μM SB. Plates were incubated in either hypoxia or normoxia. One day 2, cells were fed with Brainphys media supplemented with 1x B27, 1μg/ml doxycycline, Culture one (1:100) with feeding every other day. On day 6, plates were fixed with 4% PFA and nuclei were counterstained with DAPI, followed by imaging and statistical analysis.

Data Analysis of 2D Neural Cultures' Imaging

Fluorescence imaging of neural cultures were executed with ImageXpress microscope 20x extra-long working distance 6 days after initialization of experiments. Brightfield, DAPI and red fluorescence from POU4F2-tdTomato were captured for all treatment groups.

Multi wavelength cell scoring program was used to analyzed ratio of cells expressing POU4F2-tdTomato to total cells represented by DAPI staining. Parameters used for red fluorescence scoring were minimal width 8μm, maximal width 15μm and 100 gray levels above local background. Parameters used for DAPI staining were minimal width 10μm, maximal width 15μm and 200 gray levels above local background. Those parameters were tested to minimize counting of auto-fluorescent dead cells, while still capable of capturing most gene expressed fluorescence.

Activation of GCAMP6 slow signal in Tet-inducible NEUROG2 2D Neuron

Potassium Chloride was used to induce action potentials. 20-50mM KCl was dissolved in Brainphys Imaging Media (B.P.I. Media: #05796, STEMCELL Technology) which was used to reduce signal to noise in 2D cultures. Video recordings were shot with 200ms exposure time for GCAMP6 slow signal. After application, KCl treated neurons were washed with B.P.I. media for 3 times and maintained in 2ml of B.P.I media supplemented with 1x B27 (#17504044; Invitrogen).

Retinal Organoid Differentiation

Organoids were derived based on pre-established protocol with small modifications (Wahlin et al., 2017). IMR90.4 SIX6-eGFP POU4F2-tdTomato-MWopsin iPSCs were maintained to 50% fluency and enzymatically passaged with Accutase on day 0. An average of 125 cells were transferred to a U-bottom shaped 96 well plate in 50µl mTeSR1 plus 5µM blebbistatin and 50ng/ml TS-FGF2 (#PHG0360; Thermo Fisher). The plate was incubated in hypoxia (5% O_2 and 10% CO_2). After 24 hours, iPSCs formed cell aggregates by forced aggregation due to gravity.

On day 1, cell aggregates were fed with BE6.2 Media (DMEM (#11965; Invitrogen) supplemented with 1% B27 without vitamin A (#12587010; Invitrogen), 2x E6 supplement, 38.8 mg/L insulin (#11376497001; Roche), 128mg/L L-ascorbic acid (#A8960; Sigma), 28µg/L selenium (#S5261; Sigma), 21.4 mg/L transferrin (#T0665; Sigma) and 38.8 mg/L NaHCO3) supplemented with 2% (v/v) Matrigel (#354230; BD Biosciences) and 6µM of IWR-1e (#681669; EMD Millipore).

From day 2 to day 3, aggregates were fed with BE6.2 media supplemented with 1% (v/v) Matrigel and 3µM of IWR-1e. On day 4 to day 6, 50% exchange was performed with BE6.2 media supplemented with 1% (v/v) Matrigel and 3µM of IWR-1e. And plates were transferred to normoxia (20% O_2 and 5% CO_2) on day 5.

From day 8 to day 12, optic vesicles would start to appear and were fed every other day with BE6.2 media supplemented with 300nM SAG (#566660; EMD Millipore). On day 14, retinal organoids were transferred to non-TC treated 24 well plates and maintained in LTR media (Long Term Retinal Media: 3:1 mix of DMEM:F12 (#11965, #11765; Invitrogen) supplemented with 1x B27 (#17504044; Invitrogen), 10% (v/v) heat inactivated FBS (#16140071; Invitrogen), 1mM

pyruvate (#11360; Invitrogen), 1x NEAA (#11140; Invitrogen), 1x Glutamax (#35050061; Invitrogen) and 1mM taurine (#T-8691; Sigma)) supplemented with 300μM SAG until day 18. After day 18, retinal organoids were fed every other day with LTR media. Around day 25, retinal vesicles displaying robust SIX6-eGFP expression with promising morphology would be excised and maintained separately.

Thalamus Organoid Differentiation

Thalamus organoids were derived based on pre-established protocols with minor modifications(Xiang et al., 2019). On day 0, 50% fluent IMR90.4 iPSCs were Accutase passaged. Then, 3 to 5 thousand cells were transferred to a U-bottom shaped 96 well plates in 100μl mTeSR1 plus 5μM blebbistatin. The treatment on day 0 is different from the protocol given in the review, primarily due to difficulty in forming cell aggregate if strictly following the Xiang et al. protocol. Maintaining iPSCs in mTeSR1 and Blebbistatin on day 0 strongly improved the chance of forming compact cell aggregates. On day 1, cell aggregates were fed with TNIM (Thalamus Neural Induction Media: DMEM-F12(#11965, #11765; Invitrogen), 15% (v/v) KSR (#10828028; Gibco), 1x NEAA (#11140; Invitrogen), 1x Glutamax (#35050061; Invitrogen), and 100 mM b-Mercaptoethanol (#21985023, Gibco)) supplemented with 200 nM LDN-193189, 20 mM SB-431542, 8mg/ml Insulin. On day 2, aggregates were fed with TNIM supplemented with 100 nM LDN-193189, 10 mM SB-431542, 4mg/ml Insulin. From day 3 to day 7, 50% exchange of media was performed with TNIM supplemented with 100 nM LDN-193189, 10 mM SB-431542, 4mg/ml insulin.

On day 9, organoids were transferred to non-TC treated low attachment 24 well plate and fed with TPM (Thalamus Patterning Media: DMEM-F12, 0.15% (w/v) Dextrose, 100 mM b-Mercaptoethanol, 1x N2 supplement (#17502048; Life technologies), and 1x B27 supplement

without vitamin A) supplemented with 30 ng/ml BMP7 (#PHC7204; Gibco) and 1 mM PD325901 every other day up to day 15.

From day 17 thereafter, thalamus organoids were fed with TDM (Thalamus Differentiation Media: 1:1 mixture of DMEM-F12 and Neurobasal media (#21103049; Gibco), 0.5x N2 supplement, 1x B27, 1x MEM-NEAA, 1x Glutamax, 100 μg/ml Insulin, 50 mM b-Mercaptoethanol supplemented with 20 ng/ml BDNF (# RP-8642, Invitrogen) and 200 mM L-ascorbic acid every 3 days.

RO-ThO-CO Assembloid System

Retinal, thalamus and cortical organoids were derived independently. During fusion, three organoids were transferred to a non-TC treated low attachment 24 well plate, which were tilted ~30°. Organoids were placed down at the bottom of the well in the physiological order (RO-ThO-CO) to ensure correct direction for RGC outgrowth. Due to gravity, 3 organoids were positioned adjacent to each other at the well bottom with fusion established within 2 days. After successfully fuse, assembloids' plates were positioned horizontal and fed with Modified Muotri Lab Cortical Media 2 (Neurobasal supplemented with 1x GlutaMAX, 1x B27, 1x NEAA) daily.

As for the timing, organoids ranging from days 42 and 65 were fused with success. Organoids younger than 40 days tended to merge after fusion, losing structural integrity and cellular identity. Organoid older than 80 days were fused with success as well, but little RGC outgrowth was observed, potentially due to older RGCs being less suited for axon outgrowth.

Fixation and Immunostaining

2D Neural Cultures were fixed with 4% paraformaldehyde containing 5% sucrose for 30 minutes at room temperature and gently washed 3x with 5% sucrose in PBS. To label all cell nuclei,

we applied DAPI (1μg/ml) in 5% sucrose/PBS solution for 30 minutes at room temperature, rinsed once in PBS/sucrose and imaged using an ImageXpress fluorescent microscope.

Day 45 Thalamus organoids were fixed with 4% paraformaldehyde containing 5% sucrose for 45 minutes at room temperature, following by 3 washes with 5% sucrose. To cryoprotect tissues, fixed organoids were treated with sequential 30-minute immersion in 6.25%, 12.5% and finally 25% sucrose overnight at 4°C.

On the second day, organoids were mounted in a 1:1 mixture of OCT and 25% sucrose and sectioned at 10μm in cryostat. Slices were air dried and incubated with 1:200 primary TCF7L2 antibodies (#2565S; Cell Signaling) in blocking buffer (5% horse serum, 0.25% Tritonx100 in PBS) at 4°C overnight.

After rinsing in PBS sections were visualized with 1:1000 goat anti-rabbit AlexaFluor 488 for 1 hour and 1:1,000 DAPI. All sections were coverslipped in aquamount and stored at 4°C until imaging.

Figures

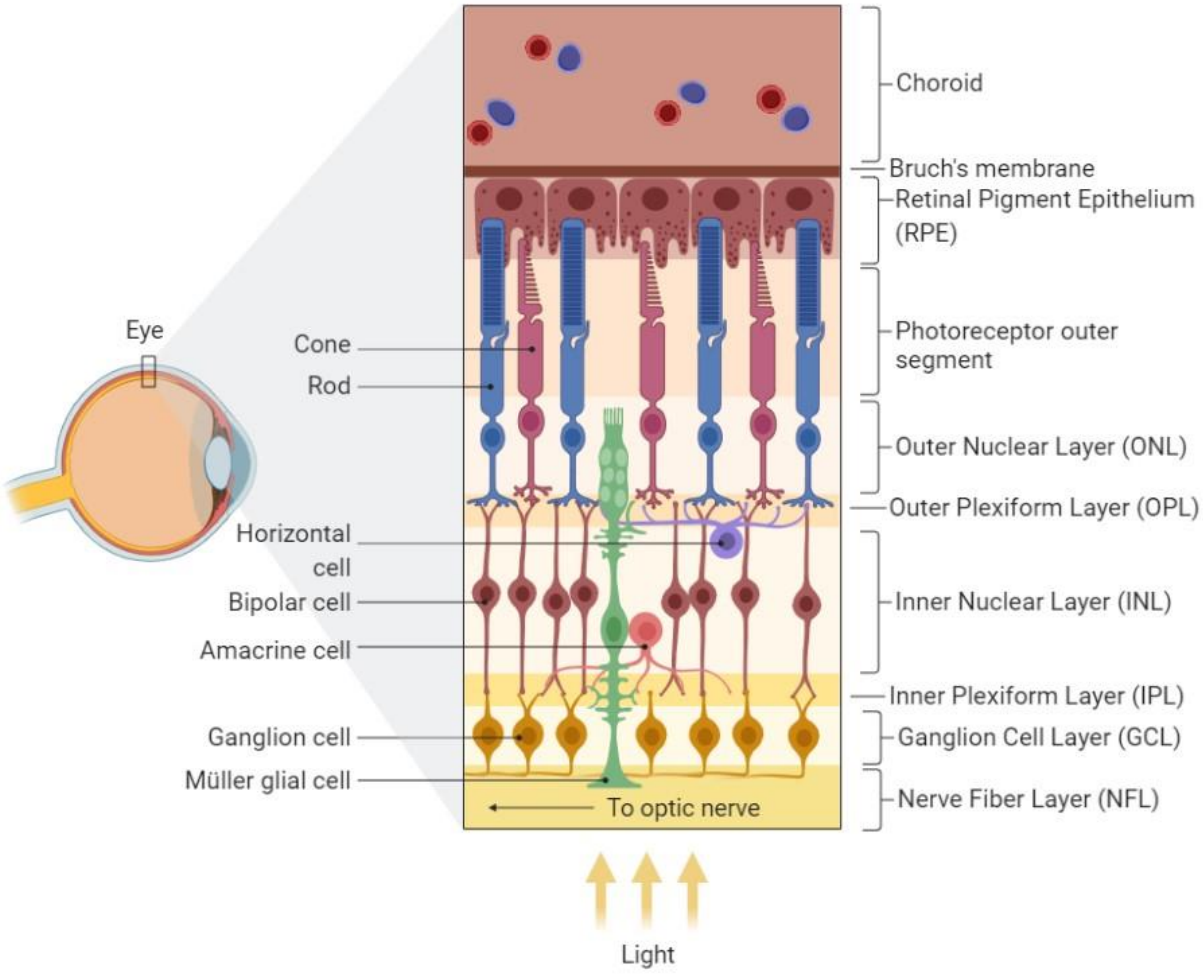

Figure 1. Retinal Cells and Laminar Structure. ONL is formed by photoreceptors' cell bodies. Innervation between photoreceptors, horizontal cells and bipolar cells forms OPL. Downward, cell bodies of horizontal cells, bipolar cells and amacrine form INL. Axon connections between bipolar cells, amacrine and RGCs form IPL. Ganglion cell bodies form GCL, and their axon bundle to form optic nerve connecting to brain. Made by Bioengineering graduate student Devansh Agarwal

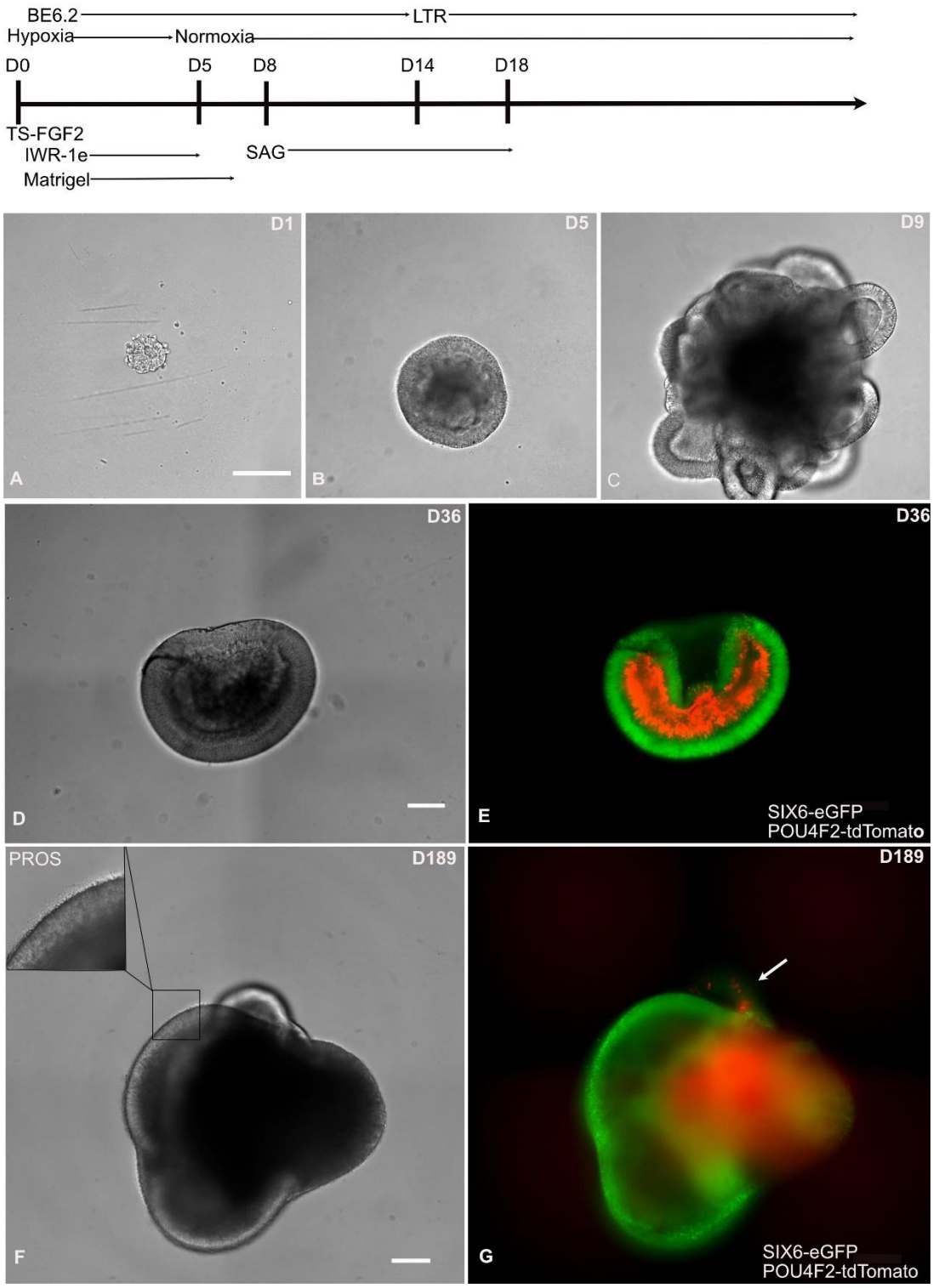

Figure 2. Live cell imaging of IMR90.4 SIX6-eGFP / POU4F2-tdTomato-MWopsin iPSC derived 3D retinal organoid development. Protocol of retinal organoid derivation was shown on the very top of the figure. Panel A-D showed retinal organoid morphology under bright field imaging from day 1 to day 36. Panel E displayed day 36 organoid had robust SIX6-eGFP and POU4F2-tdTomato RGCs' marker expression on day 36. Panel F and G showed mature day 189 organoid. Photoreceptor outer segments can be visualized already, indicated by square in Panel F. At day 189, RGCs diminished to almost non-existent, with only a few survived on a small vesicle indicated by the white arrow. Scale bars represents 200μm.

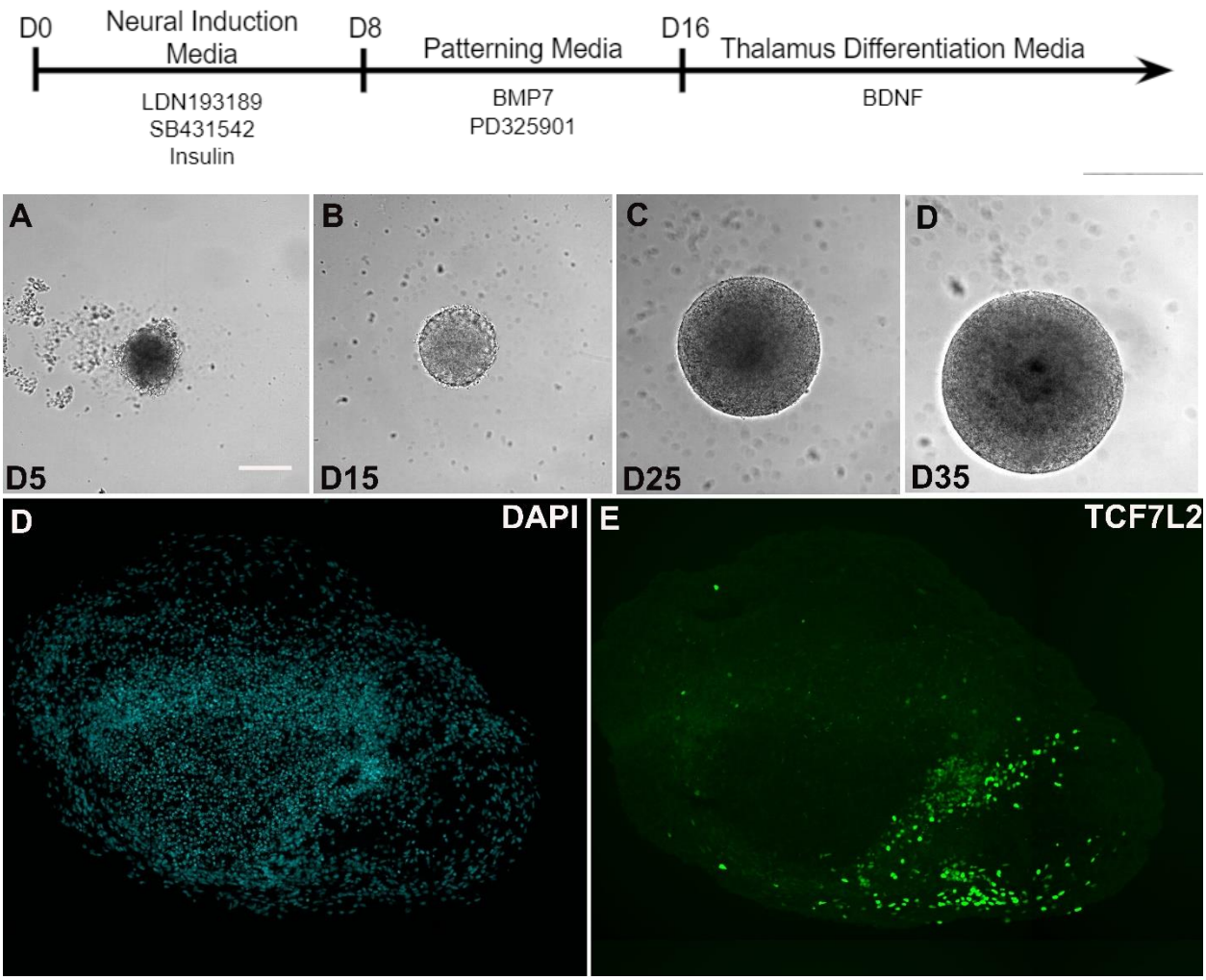

Figure 3. Development of human IMR90.4 iPSCs derived 3D thalamus organoid. Panel A-D images show the development of an individual thalamic organoid from day 5 to day 35. Panel E and F shows a D45 thalamic organoid tissue section stained with (D) DAPI nuclear and (E) TCF7L2. Scale bar represents 200μm.

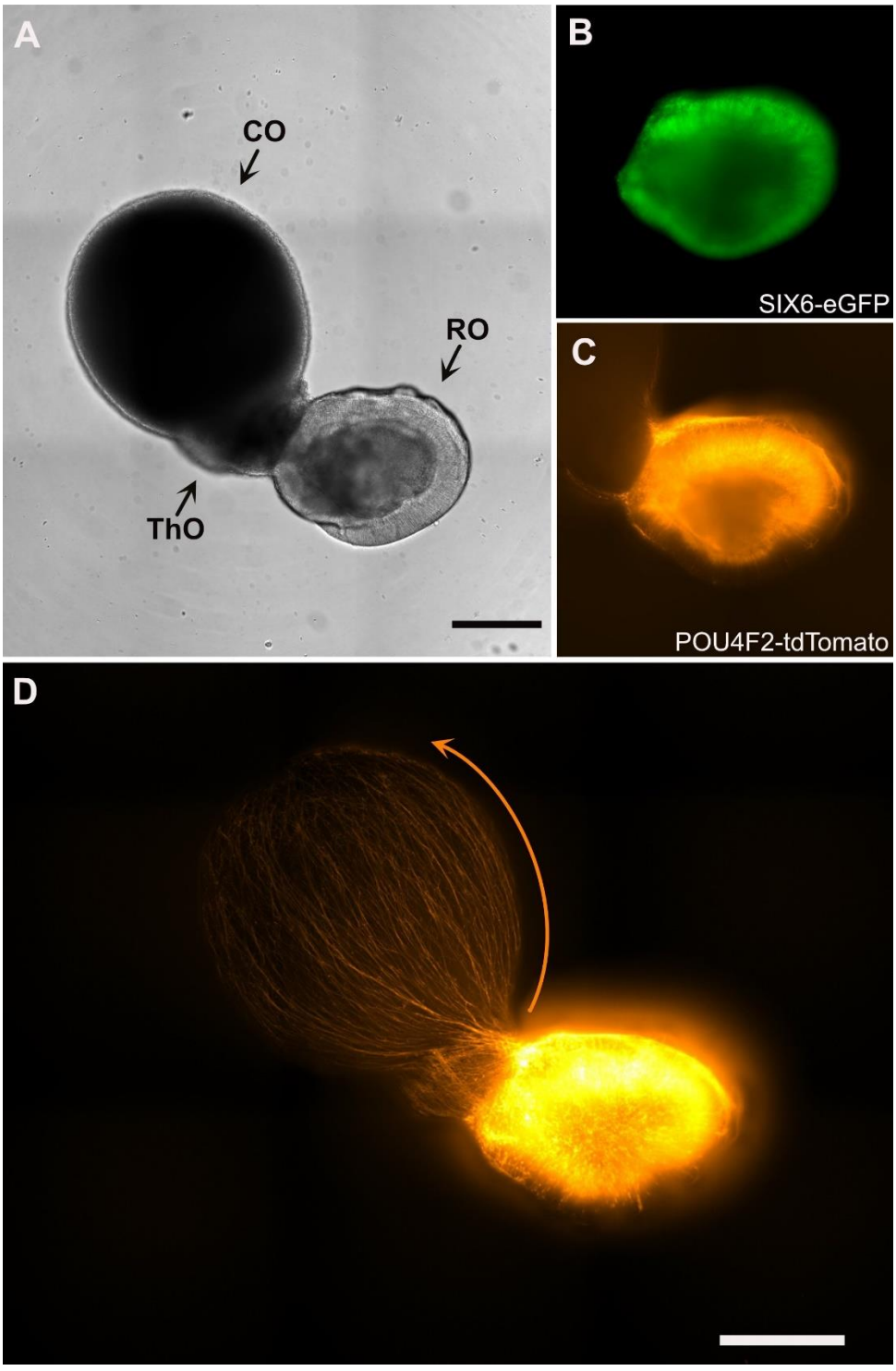

Figure 4. A Human visual circuit assembloid demonstrating outgrowth of retinal ganglion cells projecting into thalamus and cerebral organoids (A) Bright field image for assembloid with day 55 retinal (RO), day 41 thalamic (ThO) and day 60 cortical organoid (CO) fused together for 3 days (B) SIX6-p2a-eGFP expression of retinal organoid (C) POU4F2-p2a-tdTomato expression of RGCs in retinal organoid (D) Confocal z-stack live imaging showed substantial amount of RGC outgrowth into thalamic and cortical organoid, with arrow pointing in the direction of neurite outgrowth. Scale bar = 500μm.

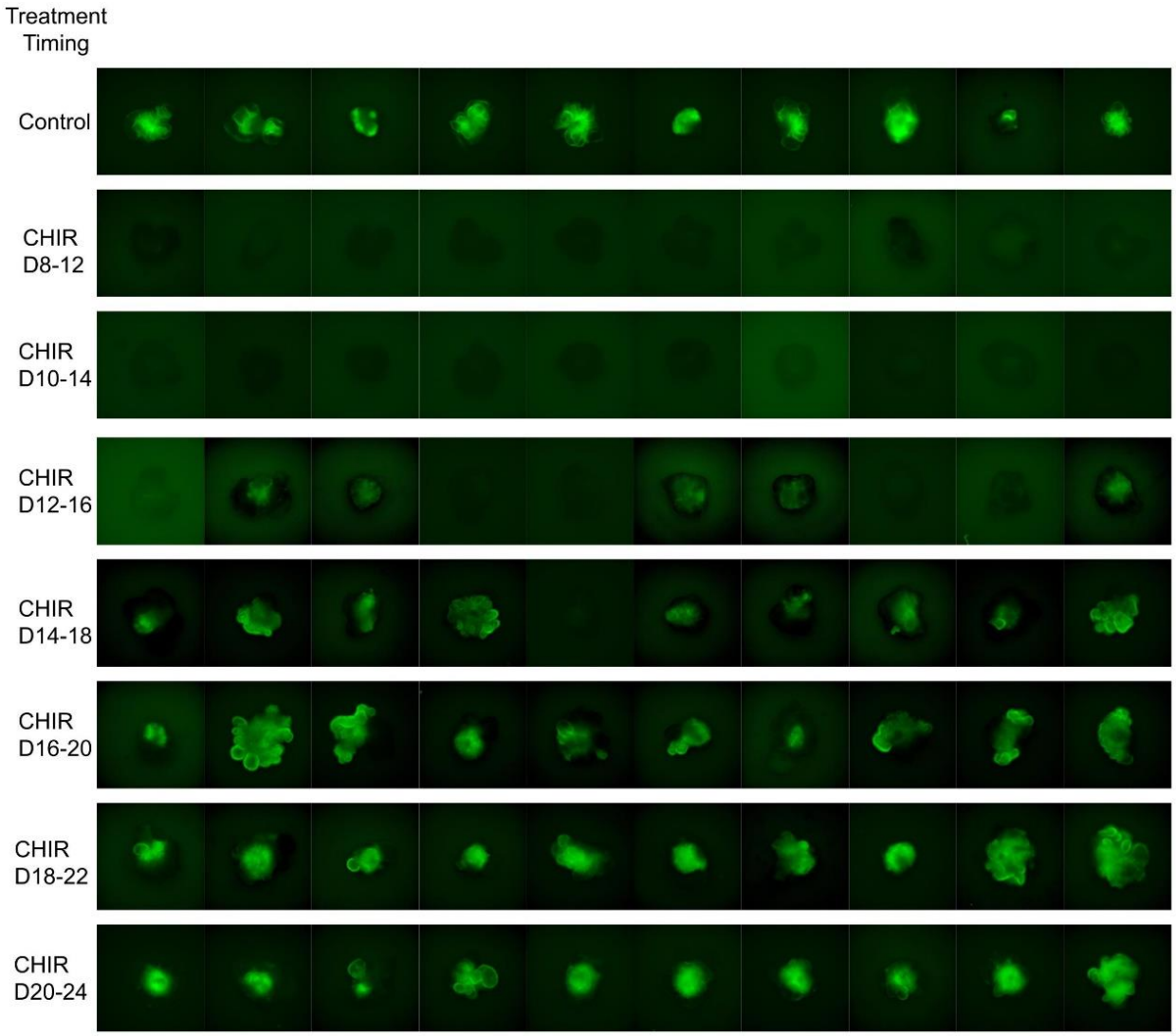

Figure 5. **Early CHIR99021 treatment completely blocks retinal development, and late CHIR99021 treatment make retinal vesicles qualitatively better.** SIX6-p2a-eGFP expression in organoids treated with CHIR99021 on different time points. The trend reflects early treatment blocks retinal vesicle formation, while treatments ranging from day 14 to day 22 significantly improve retinal vesicles' quality and SIX6-eGFP expression. The time ranges of CHIR99021 treatments of different groups were shown on the right side of figure.

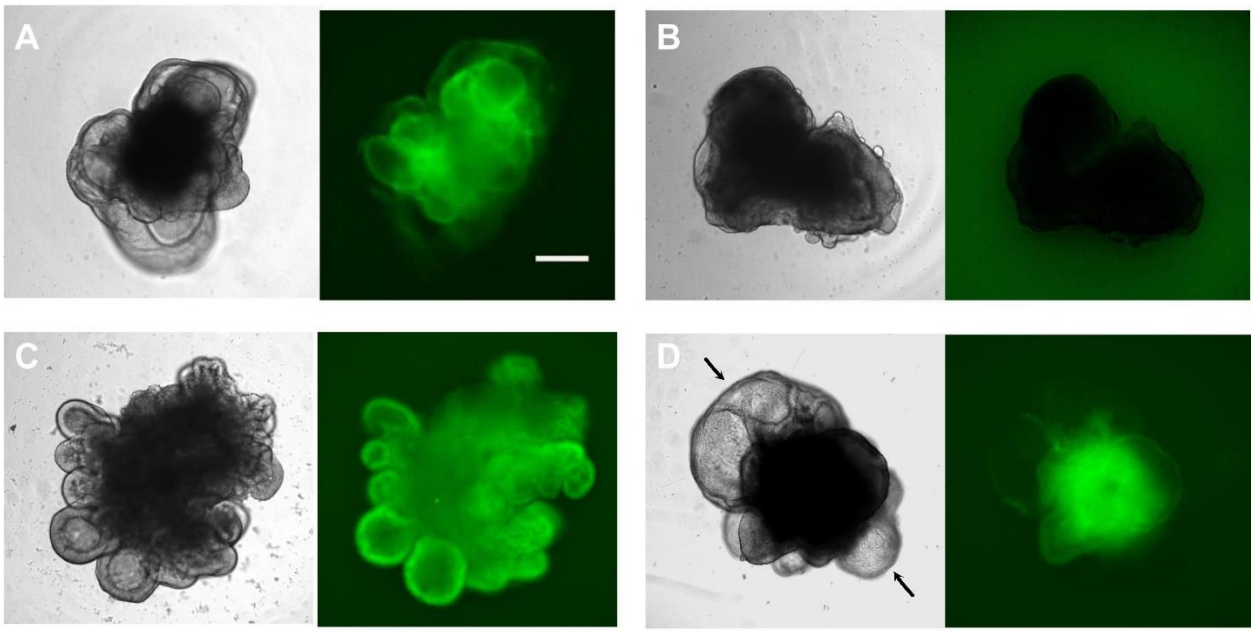

Figure 6. Representative Retinal Organoid Brightfield(left) and SIX6-p2a-eGFP(right) images of different CHIR99021 treatment groups on day 29. (A) Control group possessed some transparent vesicles(indicated by arrow) and immature recessed retinal vesicles with weak SIX6-p2a-eGFP expression (B) Early treatment of CHIR99021 from day 8-12 completely blocked SIX6-p2a-eGFP expression and retinal development (C) Late treatment of CHIR99021 from day 16-20 significantly improved retinal vesicles morphology and displayed strong SIX-p2a-eGFP expression (D) Even later CHIR treatment from day 20-24 induced more transparent non-retinal vesicles(indicated by arrows) and weak SIX6-eGFP expression, similar to control. Scale bar represents 500μm.

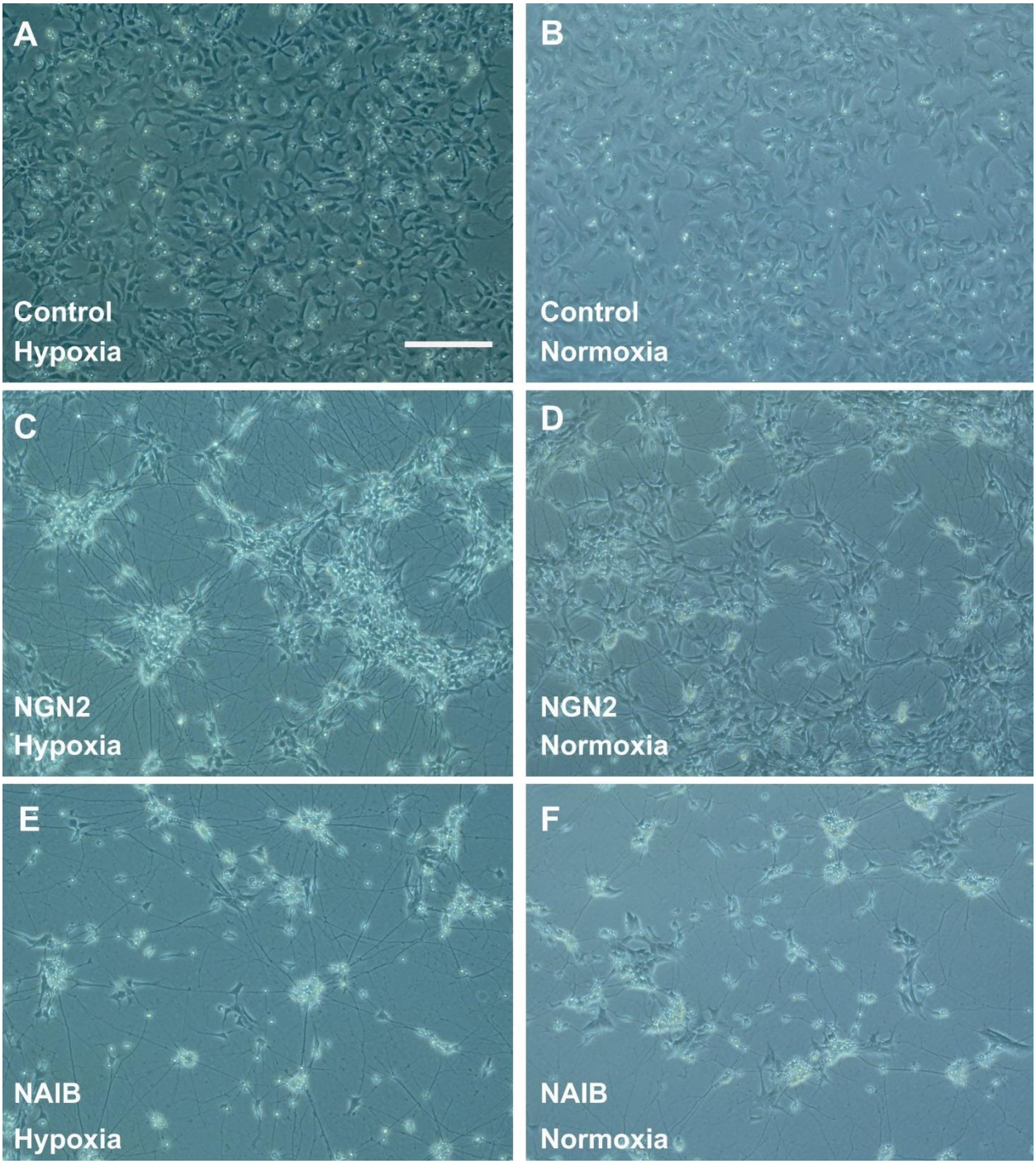

Figure 7. Comparison of control, NEUROG2 and NAIB inducible neuron 2D cultures under hypoxia and normoxia. For all three inducible cell lines treated with LDN193189 and SB431542 on day 0, no significant morphology difference was observed between normoxia and hypoxia on day 6, indicating our Tet-inducible neural culture system is robust for both conditions. Scale bar represents 200μm.

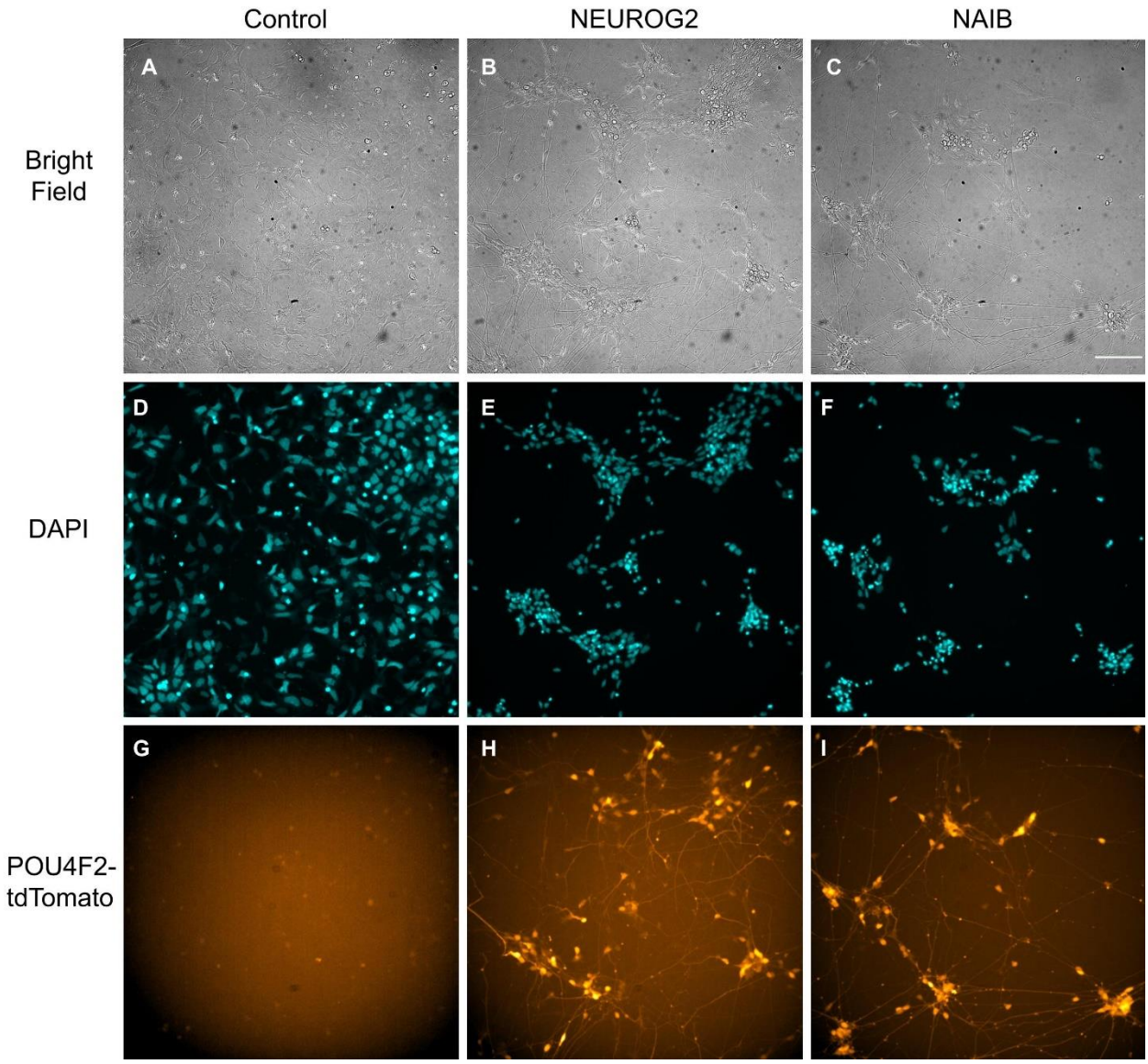

Figure 8. Fluorescence imaging of induced neurons at day 6. Figure shows 2D neuron culture in bright field (A-C), DAPI nuclear (D-F) and red fluorescence from tdTomato (G-I). Culture conditions of imaged groups were maintained in hypoxia (5% O2 and 10% CO2) and pretreated with LDN and SB one day before the experiment. Control groups showed enormous propagation with no neuron or RGC converted. NEUROG2 groups showed some propagation with decent number of RGCs converted, indicated by robust POU4F2-tdTomato expression. NAIB groups displayed very small amount of propagation, yielding a purer population of RGCs. Scale bar represents 100μm.

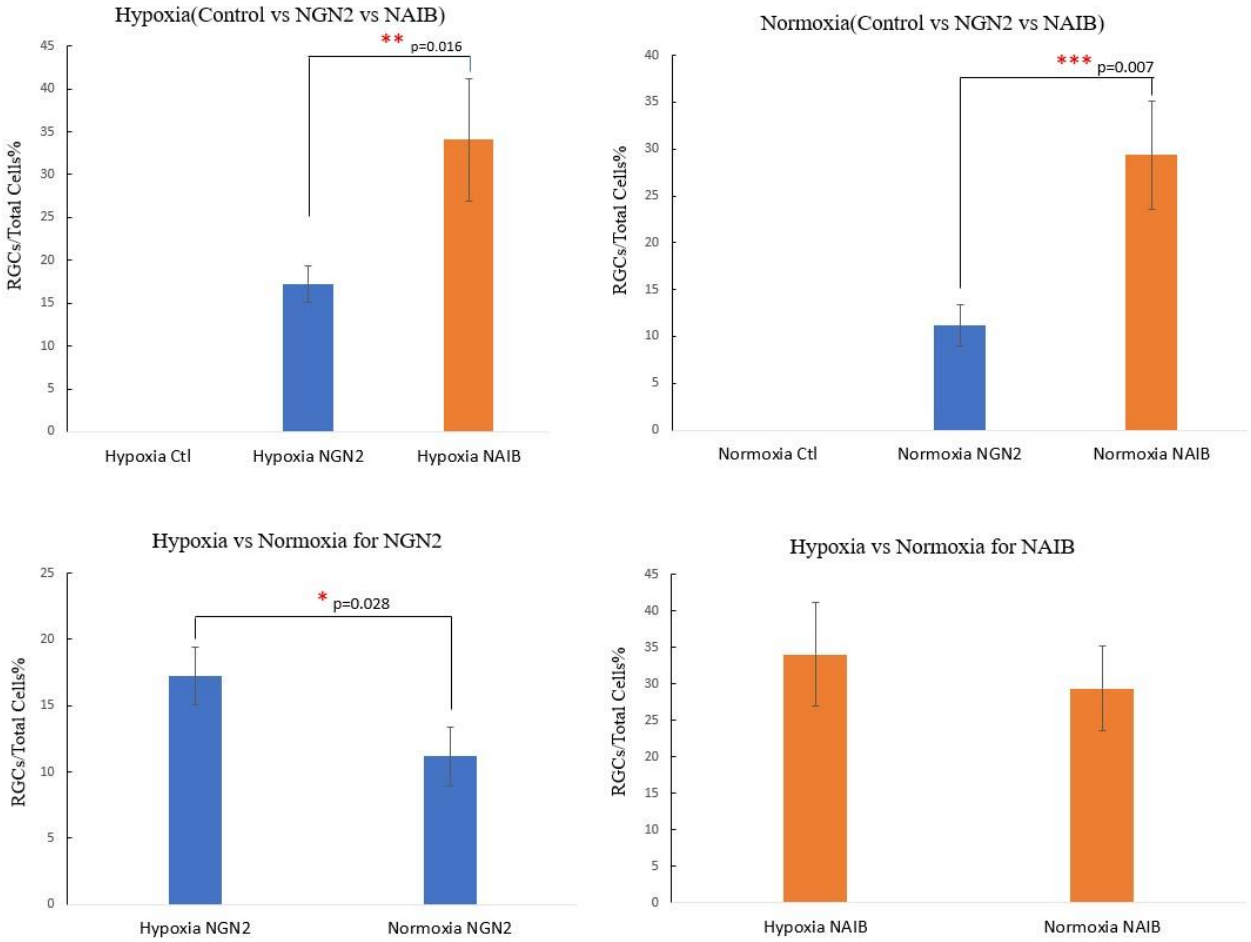

Figure 9. Efficiency of RGCs' Direction Conversion in Different Culture Conditions. In both hypoxia and normoxia culture condition, Tet-inducible NAIB cells has significantly higher efficiency of RGC conversion than that of Tet-inducible NEUROG2 cells. In hypoxia, NEUROG2 groups were significantly more efficient in RGCs' conversion than normoxia NEUROG2 group. Hypoxia NAIB cells were slightly more efficient in RGC conversion than normoxia NAIB, but with no statistical significance. P-value are generated based on two sample T-test, with $p<0.05$ selected as threshold.

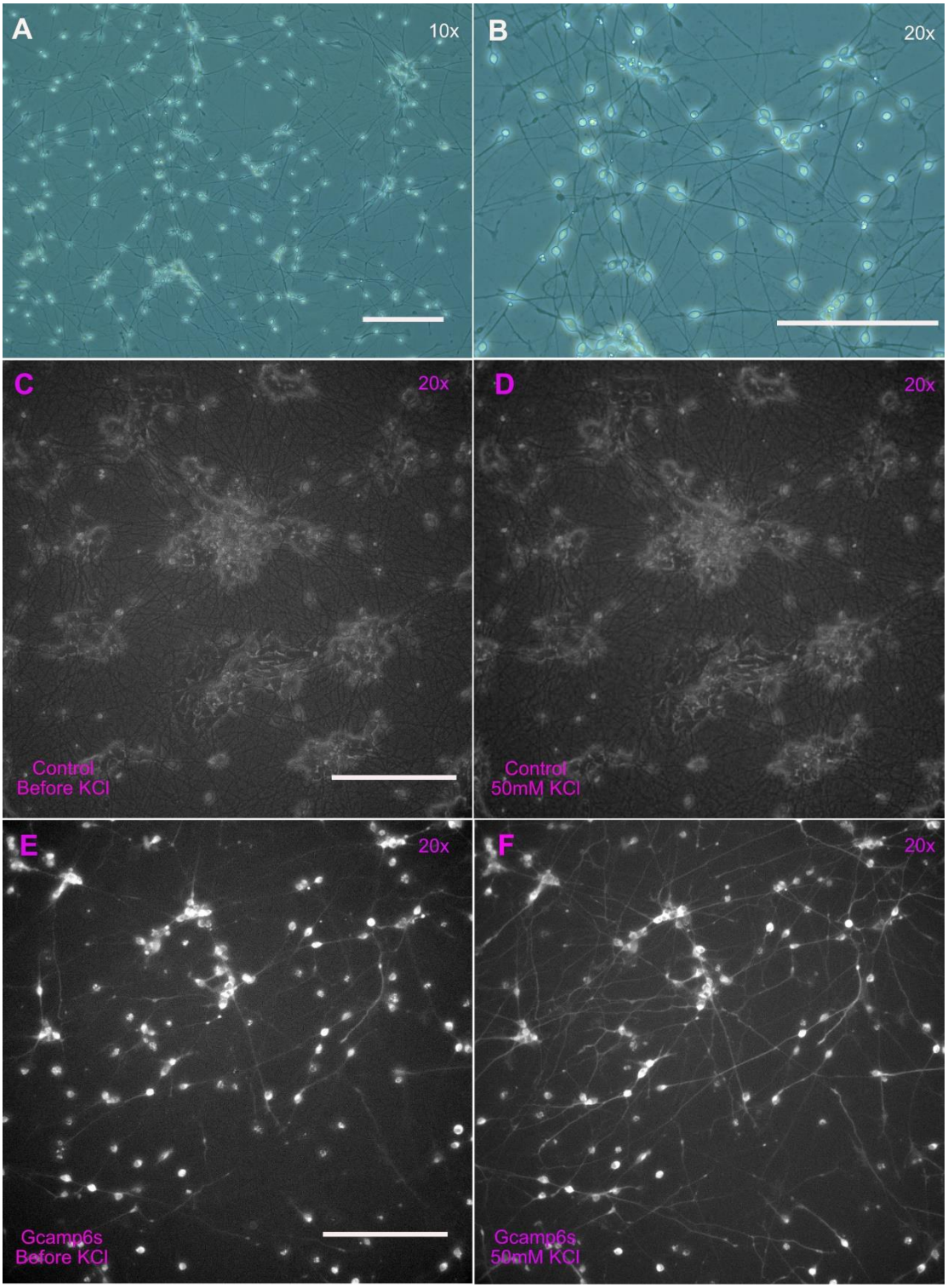

Figure 10. Gcamp6s Activation in 2D Tet-inducible Neuron Culture. (A-B) A bright field image of IMR90.4 CLYBL-Gcamp6s cells after NEUROG2 induction. These neurons show robust neurite outgrowth at day 4. **(C-D)** NEUROG2 induced neuron (without Gcamp6s) culture was selected as control group, KCl treatment induced no green fluorescence **(E)** Gcamp6s imaging before **(F)** and after 50mM KCl treatment. Robust calcium induced Gcamp6s signals represent action potential firing axons. Scale bar represents 200μm.

Table 1. Oligonucleotides Used in Optogenetic POU4F2-tdTomato-MWopsin Plasmid Transfected iPSCs Line

First Pass Genotyping Oligos Set (Insertion vs No Insertion)	
G233_hMW_unique_F	GTGGTGATGGTCCTGGCATTCTGCTT
C1103_hB3b-3p1208rev	GCCAACAAAGCAATTGAAAACTGG
Second Pass Genotyping Oligos Set (Homozygous vs Heterozygous)	
G22 Brn3b_2426NeonHomo_F	CAAACAGCCATCTCCACACTTCCTCTGAA
C1103_hB3b-3p1208rev	GCCAACAAAGCAATTGAAAACTGG

Citations

Artavanis-Tsakonas, S., Rand, M.D., Lake, R.J., 1999. Notch signaling: cell fate control and signal integration in development. Science 284, 770–776. https://doi.org/10.1126/science.284.5415.770

Badea, T.C., Cahill, H., Ecker, J., Hattar, S., Nathans, J., 2009. Distinct roles of transcription factors Brn3a and Brn3b in controlling the development, morphology, and function of retinal ganglion cells. Neuron 61, 852–864. https://doi.org/10.1016/j.neuron.2009.01.020

Berry, M.H., Holt, A., Salari, A., Veit, J., Visel, M., Levitz, J., Aghi, K., Gaub, B.M., Sivyer, B., Flannery, J.G., Isacoff, E.Y., 2019. Restoration of high-sensitivity and adapting vision with a cone opsin. Nat. Commun. 10, 1221. https://doi.org/10.1038/s41467-019-09124-x

Berson, D.M., 2003. Strange vision: ganglion cells as circadian photoreceptors. Trends Neurosci. 26, 314–320. https://doi.org/10.1016/S0166-2236(03)00130-9

Bloomfield, S.A., Xin, D., 2000. Surround inhibition of mammalian AII amacrine cells is generated in the proximal retina. J. Physiol. 523, 771–783. https://doi.org/10.1111/j.1469-7793.2000.t01-1-00771.x

Camp, J.G., Badsha, F., Florio, M., Kanton, S., Gerber, T., Wilsch-Bräuninger, M., Lewitus, E., Sykes, A., Hevers, W., Lancaster, M., Knoblich, J.A., Lachmann, R., Pääbo, S., Huttner, W.B., Treutlein, B., 2015. Human cerebral organoids recapitulate gene expression programs of fetal neocortex development. Proc. Natl. Acad. Sci. 112, 15672–15677. https://doi.org/10.1073/pnas.1520760112

Carroll, S.B., 1995. Homeotic genes and the evolution of arthropods and chordates. Nature 376, 479–485. https://doi.org/10.1038/376479a0

Chen, T.-W., Wardill, T.J., Sun, Y., Pulver, S.R., Renninger, S.L., Baohan, A., Schreiter, E.R., Kerr, R.A., Orger, M.B., Jayaraman, V., Looger, L.L., Svoboda, K., Kim, D.S., 2013. Ultrasensitive fluorescent proteins for imaging neuronal activity. Nature 499, 295–300. https://doi.org/10.1038/nature12354

Chen, Y., Stump, R.J.W., Lovicu, F.J., Shimono, A., McAvoy, J.W., 2008. Wnt signaling is required for organization of the lens fiber cell cytoskeleton and development of lens three-dimensional architecture. Dev. Biol. 324, 161–176. https://doi.org/10.1016/j.ydbio.2008.09.002

Colwell, C.S., Michel, S., Itri, J., Rodriguez, W., Tam, J., Lelièvre, V., Hu, Z., Waschek, J.A., 2004. Selective deficits in the circadian light response in mice lacking PACAP. Am. J. Physiol.-Regul. Integr. Comp. Physiol. 287, R1194–R1201. https://doi.org/10.1152/ajpregu.00268.2004

Diacou, R., Zhao, Y., Zheng, D., Cvekl, A., Liu, W., 2018. Six3 and Six6 Are Jointly Required for the Maintenance of Multipotent Retinal Progenitors through Both Positive and Negative Regulation. Cell Rep. 25, 2510-2523.e4. https://doi.org/10.1016/j.celrep.2018.10.106

Dyer, M.A., Cepko, C.L., 2000. Control of Müller glial cell proliferation and activation following retinal injury. Nat. Neurosci. 3, 873–880. https://doi.org/10.1038/78774

Elkouby, Y.M., Frank, D., 2010. Wnt/β-Catenin Signaling in Vertebrate Posterior Neural Development. Colloq. Ser. Dev. Biol. 1, 1–79. https://doi.org/10.4199/C00015ED1V01Y201007DEB004

Fedtsova, N.G., Turner, E.E., 1995. Brn-3.0 expression identifies early post-mitotic CNS neurons and sensory neural precursors. Mech. Dev. 53, 291–304. https://doi.org/10.1016/0925-4773(95)00435-1

Fuhrmann, S., Levine, E.M., Reh, T.A., 2000a. Extraocular mesenchyme patterns the optic vesicle during early eye development in the embryonic chick. Dev. Camb. Engl. 127, 4599–4609.

Fuhrmann, S., Levine, E.M., Reh, T.A., 2000b. Extraocular mesenchyme patterns the optic vesicle during early eye development in the embryonic chick. Development 127, 4599–4609. https://doi.org/10.1242/dev.127.21.4599

Guimarães, R.P. de M., Landeira, B.S., Coelho, D.M., Golbert, D.C.F., Silveira, M.S., Linden, R., de Melo Reis, R.A., Costa, M.R., 2018. Evidence of Müller Glia Conversion Into Retina Ganglion Cells Using Neurogenin2. Front. Cell. Neurosci. 12, 410. https://doi.org/10.3389/fncel.2018.00410

Hufnagel, R.B., Le, T.T., Riesenberg, A.L., Brown, N.L., 2010. Neurog2 controls the leading edge of neurogenesis in the mammalian retina. Dev. Biol. 340, 490–503. https://doi.org/10.1016/j.ydbio.2010.02.002

Hyer, J., Kuhlman, J., Afif, E., Mikawa, T., 2003. Optic cup morphogenesis requires pre-lens ectoderm but not lens differentiation. Dev. Biol. 259, 351–363. https://doi.org/10.1016/s0012-1606(03)00205-7

Jeffries, A.M., Killian, N.J., Pezaris, J.S., 2014. Mapping the primate lateral geniculate nucleus: A review of experiments and methods. J. Physiol. Paris 108, 3–10. https://doi.org/10.1016/j.jphysparis.2013.10.001

Keenan, W.T., Rupp, A.C., Ross, R.A., Somasundaram, P., Hiriyanna, S., Wu, Z., Badea, T.C., Robinson, P.R., Lowell, B.B., Hattar, S.S., n.d. A visual circuit uses complementary mechanisms to support transient and sustained pupil constriction. eLife 5, e15392. https://doi.org/10.7554/eLife.15392

Kiecker, C., Niehrs, C., 2001. A morphogen gradient of Wnt/beta-catenin signalling regulates anteroposterior neural patterning in Xenopus. Dev. Camb. Engl. 128, 4189–4201.

Kim, J.Y., Lee, J.S., Hwang, H.S., Lee, D.R., Park, C.-Y., Jung, S.J., You, Y.R., Kim, D.-S., Kim, D.-W., 2018. Wnt signal activation induces midbrain specification through direct binding of the beta-catenin/TCF4 complex to the EN1 promoter in human pluripotent stem cells. Exp. Mol. Med. 50, 1–13. https://doi.org/10.1038/s12276-018-0044-y

Kreslova, J., Machon, O., Ruzickova, J., Lachova, J., Wawrousek, E.F., Kemler, R., Krauss, S., Piatigorsky, J., Kozmik, Z., 2007. Abnormal lens morphogenesis and ectopic lens formation in the absence of β-catenin function. genesis 45, 157–168. https://doi.org/10.1002/dvg.20277

Kupfer, C., Chumbley, L., Downer, J.C., 1967. Quantitative histology of optic nerve, optic tract and lateral geniculate nucleus of man. J. Anat. 101, 393–401.

Lancaster, M.A., Renner, M., Martin, C.-A., Wenzel, D., Bicknell, L.S., Hurles, M.E., Homfray, T., Penninger, J.M., Jackson, A.P., Knoblich, J.A., 2013. Cerebral organoids model human brain development and microcephaly. Nature 501, 373–379. https://doi.org/10.1038/nature12517

Martin, P.R., 1986. The projection of different retinal ganglion cell classes to the dorsal lateral geniculate nucleus in the hooded rat. Exp. Brain Res. 62, 77–88. https://doi.org/10.1007/BF00237404

Maurer, K.A., Riesenberg, A.N., Brown, N.L., 2014. Notch signaling differentially regulates Atoh7 and Neurog2 in the distal mouse retina. Dev. Camb. Engl. 141, 3243–3254. https://doi.org/10.1242/dev.106245

McEvilly, R.J., Erkman, L., Luo, L., Sawchenko, P.E., Ryan, A.F., Rosenfeld, M.G., 1996. Requirement for Brn-3.0 in differentiation and survival of sensory and motor neurons. Nature 384, 574–577. https://doi.org/10.1038/384574a0

Mu, X., Fu, X., Beremand, P.D., Thomas, T.L., Klein, W.H., 2008. Gene-regulation logic in retinal ganglion cell development: Isl1 defines a critical branch distinct from but overlapping with Pou4f2. Proc. Natl. Acad. Sci. 105, 6942–6947. https://doi.org/10.1073/pnas.0802627105

Nadal-Nicolás, F.M., Jiménez-López, M., Sobrado-Calvo, P., Nieto-López, L., Cánovas-Martínez, I., Salinas-Navarro, M., Vidal-Sanz, M., Agudo, M., 2009. Brn3a as a Marker of Retinal Ganglion Cells: Qualitative and Quantitative Time Course Studies in Naïve and Optic Nerve–Injured Retinas. Invest. Ophthalmol. Vis. Sci. 50, 3860–3868. https://doi.org/10.1167/iovs.08-3267

Nakatsu, M.N., Ding, Z., Ng, M.Y., Truong, T.T., Yu, F., Deng, S.X., 2011. Wnt/β-Catenin Signaling Regulates Proliferation of Human Cornea Epithelial Stem/Progenitor Cells. Invest. Ophthalmol. Vis. Sci. 52, 4734–4741. https://doi.org/10.1167/iovs.10-6486

Pierrot-Deseilligny, C., Müri, R.M., Ploner, C.J., Gaymard, B., Rivaud-Péchoux, S., 2003. Cortical control of ocular saccades in humans: a model for motricity, in: Progress in Brain Research, Neural Control of Space Coding and Action Production. Elsevier, pp. 3–17. https://doi.org/10.1016/S0079-6123(03)42003-7

Pokorny, J., 2011. Review: steady and pulsed pedestals, the how and why of post-receptoral pathway separation. J. Vis. 11, 1–23. https://doi.org/10.1167/11.5.7

Pollak, J., Wilken, M.S., Ueki, Y., Cox, K.E., Sullivan, J.M., Taylor, R.J., Levine, E.M., Reh, T.A., 2013. ASCL1 reprograms mouse Muller glia into neurogenic retinal progenitors. Dev. Camb. Engl. 140, 2619–2631. https://doi.org/10.1242/dev.091355

Quadrato, G., Brown, J., Arlotta, P., 2016. The promises and challenges of human brain organoids as models of neuropsychiatric disease. Nat. Med. 22, 1220–1228. https://doi.org/10.1038/nm.4214

Sato, T., Vries, R.G., Snippert, H.J., van de Wetering, M., Barker, N., Stange, D.E., van Es, J.H., Abo, A., Kujala, P., Peters, P.J., Clevers, H., 2009. Single Lgr5 stem cells build crypt-villus structures in vitro without a mesenchymal niche. Nature 459, 262–265. https://doi.org/10.1038/nature07935

Setia, H., Muotri, A.R., 2019. Brain organoids as a model system for human neurodevelopment and disease. Semin. Cell Dev. Biol. 95, 93–97. https://doi.org/10.1016/j.semcdb.2019.03.002

Smith, A.N., Miller, L.-A.D., Song, N., Taketo, M.M., Lang, R.A., 2005. The duality of β-catenin function: A requirement in lens morphogenesis and signaling suppression of lens fate in periocular ectoderm. Dev. Biol. 285, 477–489. https://doi.org/10.1016/j.ydbio.2005.07.019

Thoreson, W.B., Mangel, S.C., 2012. Lateral interactions in the outer retina. Prog. Retin. Eye Res. 31, 407–441. https://doi.org/10.1016/j.preteyeres.2012.04.003

Trujillo, C.A., Gao, R., Negraes, P.D., Gu, J., Buchanan, J., Preissl, S., Wang, A., Wu, W., Haddad, G.G., Chaim, I.A., Domissy, A., Vandenberghe, M., Devor, A., Yeo, G.W., Voytek, B., Muotri, A.R., 2019. Complex Oscillatory Waves Emerging from Cortical Organoids Model Early Human Brain Network Development. Cell Stem Cell 25, 558-569.e7. https://doi.org/10.1016/j.stem.2019.08.002

Veien, E.S., Rosenthal, J.S., Kruse-Bend, R.C., Chien, C.-B., Dorsky, R.I., 2008. Canonical Wnt signaling is required for the maintenance of dorsal retinal identity. Development 135, 4101–4111. https://doi.org/10.1242/dev.027367

Wahlin, K.J., Maruotti, J.A., Sripathi, S.R., Ball, J., Angueyra, J.M., Kim, C., Grebe, R., Li, W., Jones, B.W., Zack, D.J., 2017. Photoreceptor Outer Segment-like Structures in Long-Term 3D Retinas from Human Pluripotent Stem Cells. Sci. Rep. 7, 766. https://doi.org/10.1038/s41598-017-00774-9

Wang, S.W., Mu, X., Bowers, W.J., Kim, D.-S., Plas, D.J., Crair, M.C., Federoff, H.J., Gan, L., Klein, W.H., 2002. Brn3b/Brn3c double knockout mice reveal an unsuspected role for Brn3c in retinal ganglion cell axon outgrowth. Development 129, 467–477. https://doi.org/10.1242/dev.129.2.467

Wohl, S.G., Hooper, M.J., Reh, T.A., 2019. MicroRNAs miR-25, let-7 and miR-124 regulate the neurogenic potential of Müller glia in mice. Development 146. https://doi.org/10.1242/dev.179556

Wu, F., Kaczynski, T.J., Sethuramanujam, S., Li, R., Jain, V., Slaughter, M., Mu, X., 2015. Two transcription factors, Pou4f2 and Isl1, are sufficient to specify the retinal ganglion cell fate. Proc. Natl. Acad. Sci. 112, E1559–E1568. https://doi.org/10.1073/pnas.1421535112

Xiang, M., 1998. Requirement for Brn-3b in early differentiation of postmitotic retinal ganglion cell precursors. Dev. Biol. 197, 155–169. https://doi.org/10.1006/dbio.1998.8868

Xiang, M., Zhou, L., Macke, J., Yoshioka, T., Hendry, S., Eddy, R., Shows, T., Nathans, J., 1995. The Brn-3 family of POU-domain factors: primary structure, binding specificity,

and expression in subsets of retinal ganglion cells and somatosensory neurons. J. Neurosci. 15, 4762–4785. https://doi.org/10.1523/JNEUROSCI.15-07-04762.1995

Xiang, Y., Tanaka, Y., Cakir, B., Patterson, B., Kim, K.-Y., Sun, P., Kang, Y.-J., Zhong, M., Liu, X., Patra, P., Lee, S.-H., Weissman, S.M., Park, I.-H., 2019. hESC-Derived Thalamic Organoids Form Reciprocal Projections When Fused with Cortical Organoids. Cell Stem Cell 24, 487-497.e7. https://doi.org/10.1016/j.stem.2018.12.015

Xu, X., Ichida, J.M., Allison, J.D., Boyd, J.D., Bonds, A.B., Casagrande, V.A., 2001. A comparison of koniocellular, magnocellular and parvocellular receptive field properties in the lateral geniculate nucleus of the owl monkey (Aotus trivirgatus). J. Physiol. 531, 203–218. https://doi.org/10.1111/j.1469-7793.2001.0203j.x

Zhou, C.-J., Molotkov, A., Song, L., Li, Y., Pleasure, D.E., Pleasure, S.J., Wang, Y.-Z., 2008. Ocular coloboma and dorsoventral neuroretinal patterning defects in Lrp6 mutant eyes. Dev. Dyn. 237, 3681–3689. https://doi.org/10.1002/dvdy.21770

Zou, M., Li, S., Klein, W.H., Xiang, M., 2012. Brn3a/Pou4f1 Regulates Dorsal Root Ganglion Sensory Neuron Specification and Axonal Projection into the Spinal Cord. Dev. Biol. 364, 114–127. https://doi.org/10.1016/j.ydbio.2012.01.021